21st Australasian Fluid Mechanics Conference
Adelaide, Australia
10-13 December 2018

Heat and mass transport in geostrophic horizontal convection with surface wind stress

T. Sohail[1,2], C. A. Vreugdenhil[3], B. Gayen[1] and A. McC. Hogg[1,2]

[1]Research School of Earth Sciences
The Australian National University, Canberra, Australian Capital Territory, 2600, Australia

[2]ARC Centre of Excellence in Climate Extremes
The Australian National University, Canberra, Australian Capital Territory, 2600, Australia

[3]Department of Applied Mathematics and Theoretical Physics
University of Cambridge, Cambridge, United Kingdom

Abstract

Direct Numerical Simulations are conducted to investigate heat and mass transport of flow with buoyancy forcing and surface wind stress. We use a re-entrant channel model with thermal and mechanical forcing similar to the Southern Ocean, with increasing surface wind stress. The model fully characterises convection and turbulence in the fluid. The presence of convection appears to significantly enhance the buoyancy-driven overturning, resulting in an overturning cell which dominates the flow field compared with a relatively shallow and weak wind-driven cell. The vertical heat transport also indicates that the majority of vertical advective heat transport occurs in the convective zone, with strong upwelling of heat in this region. These results indicate that the presence of convection significantly enhances the impact of buoyancy forcing in driving mass and heat transport.

Introduction

The Meridional Overturning Circulation (MOC) is a key modulator of global climate, contributing to heat uptake and poleward heat transfer [10] and anthropogenic carbon dioxide absorption [8]. The MOC is characterised by downwelling of cold, negatively buoyant waters in the Southern Ocean and Northern oceans and a gradual upwelling of abyssal waters. In the Southern Ocean, a deep limb of downwelling water, known as the Antarctic Bottom Water (AABW) forms the lower of two overturning cells [4]. The AABW is a buoyancy-driven cell driven by surface buoyancy fluxes and interior mixing. The sensitivity of this buoyancy-driven cell to surface forcing, including wind and buoyancy, has been modelled in eddy-permitting ocean models [1,5,6]. These models have shown some sensitivity of the AABW formation to wind stress, with increasing wind stress resulting in stronger overturning circulation. However, these modelling studies no not include convection and turbulence, as they are typically large-scale hydrostatic models, in which vertical transport is inferred rather than explicitly resolved. Vertical resolution in particular is very coarse, so the small-scale structures associated with convection are not resolved. As a result, the impact of small scales of motion on the overturning has not been studied.

The advective heat transport, and particularly the vertical structure of heat transport, has not been studied the presence of convection. Prior work investigating poleward heat transport has used relatively coarse-resolution models [2,3], and therefore has not been able to accurately estimate the variability of vertical heat transport with changing wind forcing.

Method

We investigate the impact of turbulence and convection on the overturning circulation and vertical heat transport using a Direct Numerical Simulation (DNS) with a re-entrant channel configuration. Following prior work, [9], we impose a surface meridional temperature gradient to trigger horizontal convection, along with a surface velocity shear to simulate surface wind stress (see figure 1).

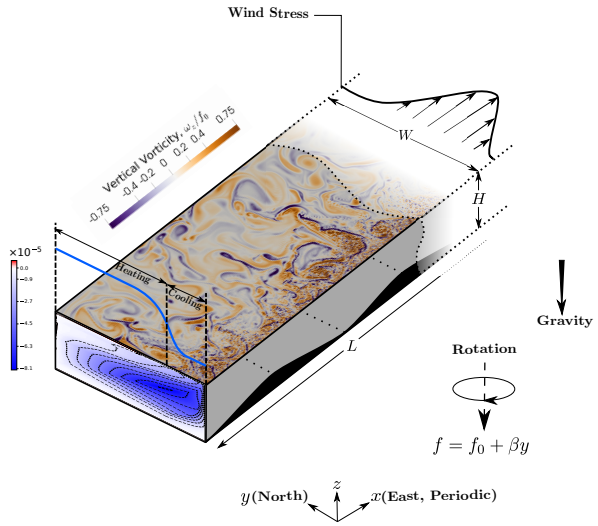

Figure 1. Domain overview for simulations conducted. The surface buoyancy forcing is shown in blue, and the surface wind stress in black. The top surface is the instantaneous normalised vertical component of relative vorticity, $\hat{\omega} = \omega/f_0$, and the side plane shows the normalised depth-density streamfunction, mapped onto the latitude-depth domain. The schematic has been truncated in the zonal direction.

The model lies in the geostrophic regime and the forcing configuration is tuned to be geophysically relevant with the help of the following non-dimensional parameters:

$$Ra = \frac{g^* W^3}{\nu\kappa}, E = \frac{\nu}{f_0 W^2}, Pr = \frac{\nu}{\kappa}, S = \frac{\tau_{max}}{\rho_0 g^* H},$$
$$\hat{\beta} = \frac{\beta W}{f_0}, B = \frac{L}{W}, D = \frac{H}{W}. \quad (1)$$

where Ra is the Rayleigh number, E is the Ekman number, Pr is the Prandtl number, S non-dimensionalises surface wind stress, $\hat{\beta}$ is the non-dimensionalised beta plane and B and D are the relevant aspect ratios. Here, g^* is the reduced gravity, defined as $g^*=g\alpha\Delta T$, based on thermal expansion coefficient α, gravitational acceleration g and the temperature difference at the surface, ΔT. W, L and H are the model dimensions corresponding to the y (northward, meridional), x (eastward,

zonal) and z (depth) directions. The Coriolis parameter is f_0 at the Southern boundary (y=0), ν is molecular viscosity, κ is molecular diffusivity, β is the latitudinal variance of the Coriolis parameter, ρ_0 is the reference density and τ_{max} is the maximum zonal wind stress.

The model uses molecular viscosity and diffusivity, and has no parameterisations, resolving the local Kolmogorov scale at all grid points. The model resolution is $W \times L \times H = 513 \times 1024 \times 258$. The system is spun up to thermal equilibrium, defined as the state when the positive and negative surface diffusive heat fluxes are within 5% of each other. We conduct 4 experiments with increasing wind stress, S, as detailed in Table 1.

Case	S
A	0
B	4.44×10^{-5}
C	8.89×10^{-5}
D	1.77×10^{-4}

Table 1. Range of wind stress imposed on the model for Cases A - D.

Note that for all cases, $Ra \sim 10^{12}, E \sim 10^{-7}, Pr \sim 5, \hat{\beta} = 0.03, D = 0.4$ and $B = 5$.

Results

The model resolves fine-scale structures in the flow, as can be seen in figure 1. The top vorticity surface shows fine-scale eddies and vortical structures consistent with convection along the southern edge of the domain. Moving northwards, filaments and jets analogous to the Antarctic Circumpolar Current (ACC) are visible. The complex feedbacks between these flow processes and the resulting overturning circulation and heat transport are analysed in this study.

In order to visualise the overturning circulation in the simulation runs, we rely on a diagnostic tool known as the depth-density streamfunction. The depth-density streamfunction, $\Psi_{\rho,z}$ is defined as the vertical transport within density classes [7]:

$$\Psi_{\rho,z} = -\frac{1}{\Delta t}\int\int\int_{\rho_{bin}\geq\rho} w(x,y,z,t)dxdydt \tag{2}$$

where w is vertical velocity, t is time and ρ_{bin} is the range of density classes over which w is integrated. The utility of this type of streamfunction is that it enables us to distinguish between the thermally-direct, or buoyancy-driven flow, and the thermally-indirect, or wind-driven overturning [7].

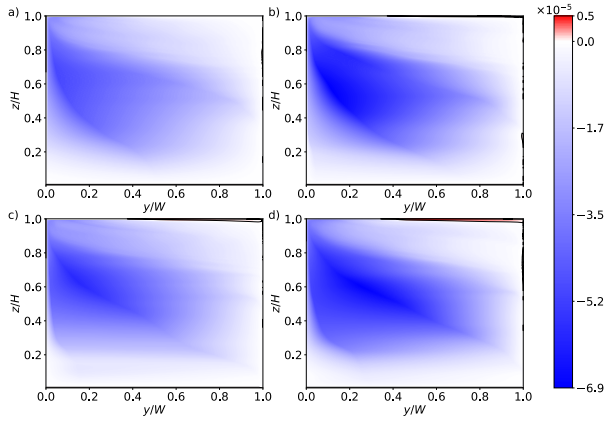

Figure 2. Depth-density streamfunction, $\Psi_{\rho,z}$ for Cases A-D (corresponding to a) – d) respectively) in the meridional y-z plane.

The depth-density streamfunction for Cases A-D are mapped onto depth-latitude co-ordinates, as shown in Figure 2. The large thermally-direct buoyancy-driven cell (in blue) is evident in all of the plots. This overturning cell does not appear to vary as a function of increasing wind stress, with the magnitude and spatial variance of the cell remaining constant. The wind-driven cell (in red) is relatively shallow and appears to be much weaker than the buoyancy-driven cell for all cases, though it does deepen and strengthen at the extreme cases of S (see figure 2d).

The depth-density streamfunction, $\Psi_{\rho,z}$ can be manipulated further to get an indication of vertical heat transfer in the models, termed as the Heatfunction, H [3]:

$$H = \int_{T_{bin}\leq T} \Psi_{T,z}dT = A\int_{\rho_{bin}\geq\rho} \Psi_{\rho,z}d\rho \tag{3}$$

where A is some constant to convert from density to temperature.

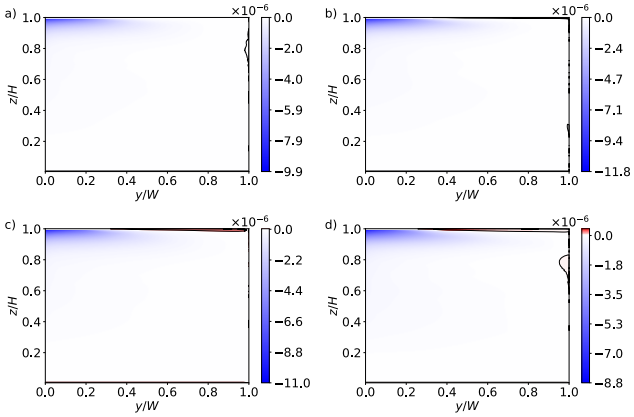

Figure 3. Heatfunction, H for Cases A-D (corresponding to a) – d) respectively) in the meridional y-z plane.

Figure 3 shows the variance in the vertical heat transport, H, with increasing S. The majority of downward flux of heat (i.e, cold water sinking) occurs at the Southern boundary where convection is active. Therefore, convection is responsible for the majority of vertical heat fluxes in this system. As S increases, H does not appear to vary significantly. A relatively small region of positive flux of negative heat (in red) can be attributed to Ekman pumping drawing the heat signal downwards. However, this region is small and of relatively low magnitude.

Discussion and Conclusions

A convection-resolving model with horizontal convection and surface wind stress is used to investigate mass and heat transport in the Southern Ocean. In a convectively-driven system, the buoyancy-driven cell (analogous to the AABW) is extremely large and of relatively high magnitude. This indicates that convection may be enhancing AABW formation in the Southern Ocean. The wind-driven overturning, on the other hand, is surface-isolated and relatively weak. The wind-driven cell may be suppressed by the relatively strong convection and anti-clockwise overturning circulation associated with the buoyancy-driven cell. The vertical heat transport shows a similarly large signature of the buoyancy forcing. The majority

of heat transport in the system is positive heat flux in the convective region. These results have major implications on understanding of the effect of turbulence on the abyssal and upper overturning circulation in the Southern Ocean.

Acknowledgements

Numerical simulations were conducted on the Australian National Computational Infrastructure (NCI), ANU, which is supported by the Commonwealth of Australia. This research was supported by the Australian Research Council grant DP140103706.

References

[1] Abernathy, A., Marshall, J. & Ferreira, D., The Dependence of Southern Ocean Meridional Overturning on Wind Stress, *Journal of Physical Oceanography*, **41**, 2011, 2261-2278.

[2] Boccaletti, G., Ferrari, R., Adcroft, A., Ferreira, D., & Marshall, J., The vertical structure of ocean heat transport. *Geophysical Research Letters*, **32**, LI0603, 2005.

[3] Ferrari, R., & Ferreira, D., What processes drive ocean heat transport?, *Ocean Modelling*, **38**, 2011, 171-186.

[4] Marshall, J., & Speer, K., Closure of the meridional overturning circulation through Southern Ocean upwelling, *Nature Geoscience*, **5**, 2012, 171 – 180

[5] Morrison, A. K. & Hogg, A. McC., On the Relationship between Southern Ocean Overturning and ACC Transport, *Journal of Physical Oceanography*, **43**, 2012, 140-148.

[6] Munday, D. R., Johnson, H. L. & Marshall, D. P., Eddy Saturation of Equilibrated Circumpolar Currents. *Journal of Physical Oceanography*, **43**, 2013, 507-532.

[7] Nycander, J., Nilsson, J., Döös, K. & Broström, G., Thermodynamic Analysis of Ocean Circulation, *Journal of Physical Oceanography*, **37**, 2007, 2038-2052.

[8] Sabine, C. L., Feely, R.A., Gruber, N., Key, R.M., Lee, K., Bullister, J.L., Wanninkhof, R., Wong, C.S., Wallace, D.W.R., Tilbrook, B., Millero, F.J., Peng, T., Kozyr, A., Ono, T., Rios, A.F., The oceanic sink for anthropogenic CO_2, *Science*, **305**, 2004, 367-371.

[9] Sohail, T., Gayen, B. & Hogg, A. McC., Convection drives mixing in the Southern Ocean, G*eophysical Research Letters*, **45**, 2018, 1-10.

[10] Trenberth, K. E. & Caron, J. M., Estimates of Meridional Atmosphere and Ocean Heat Transports, *Journal of Physical Oceanography*, **14**, 2001, 3433-3443